Evolution of a band insulating phase from a correlated metallic phase

Kalobaran Maiti,* Ravi Shankar Singh, and V.R.R. Medicherla
Department of Condensed Matter Physics and Materials' Science,
Tata Institute of Fundamental Research, Homi Bhabha Road, Colaba, Mumbai - 400 005, INDIA
(Dated: February 1, 2008)

We investigate the evolution of the electronic structure in $SrRu_{1-x}Ti_xO_3$ as a function of x using high resolution photoemission spectroscopy, where $SrRuO_3$ is a weakly correlated metal and $SrTiO_3$ is a band insulator. The surface spectra exhibit a metal-insulator transition at $x = 0.5$ by opening up a soft gap. A hard gap appears at higher x values consistent with the transport properties. In contrast, the bulk spectra reveal a pseudogap at the Fermi level, and unusual evolution exhibiting an apparent broadening of the coherent feature and subsequent decrease in intensity of the lower Hubbard band with the increase in x. Interestingly, the first principle approaches are found to be sufficient to capture anomalous evolutions at high energy scale. Analysis of the spectral lineshape indicates strong interplay between disorder and electron correlation in the electronic properties of this system.

PACS numbers: 71.10.Hf, 71.20.-b, 71.30.+h

The investigation of the role of electron correlation in various electronic properties is a paradigmatic problem in solid state physics. Numerous experimental and theoretical studies are being performed on correlated electron systems revealing exotic phenomena such as high temperature superconductivity, giant magnetoresistance *etc.* Electron correlation essentially localizes the valence electrons leading the system towards insulating phase. Correlation induced insulators, known as *Mott insulators* are characterized by a gapped electronic excitations in a system where effective single particle approaches provide a metallic ground state. The *band insulators* represent insulating phase described within the single particle approaches. Strikingly, some recent theoretical studies reveal a correlation induced metallic ground state in a band insulator using ionic Hubbard model [1, 2, 3, 4]. Such unusual transition has been observed in two dimensions by tuning effective electron correlation strength, U/W (U = electron-electron Coulomb repulsion strength, W = bandwidth) and the local potential, Δ.

In order to realize such effect experimentally, we investigate the evolution of the electronic structure in $SrRu_{1-x}Ti_xO_3$ as a function of x, where the end members, $SrRuO_3$ and $SrTiO_3$ are correlated ferromagnetic metal and band insulator, respectively. Ti remains in tetravalent state in the whole composition range having no electron in the $3d$ band[5, 6]. Thus, in addition to the introduction of disorder in the Ru-O sublattice, Ti-substitution at the Ru-sites dilutes Ru-O-Ru connectivity leading to a reduction in Ru $4d$ bandwidth, W and hence, U/W will increase. Transport measurements[7] exhibit plethora of novel phases such as correlated metal ($x \sim 0.0$), disordered metal ($x \sim 0.3$), Anderson insulator ($x \sim 0.5$), soft Coulomb gap insulator ($x \sim 0.6$), disordered correlated insulator ($x \sim 0.8$), and band insulator ($x = 1.0$).

In this study, we have used high resolution photoemission spectroscopy to probe the density function in the vicinity of the Fermi level, ϵ_F and at higher energy scale as well. Considering the fact that escape depth of the photoelectrons is small, we have extracted the surface and bulk spectra in every case by varying the surface sensitivity of the technique. The surface spectra exhibit signature of disorder at lower x values in $SrRu_{1-x}Ti_xO_3$, a metal-insulator transition exhibiting a soft gap at ϵ_F for $x = 0.5$ and a hard gap for higher x. The bulk spectra, on the other hand, reveal an unusual spectral weight transfer and signature of a *pseudogap* at ϵ_F at higher x.

Photoemission measurements were performed using Gammadata Scienta analyzer, SES2002 and monochromatized photon sources. The energy resolution for x-ray photoemission (XP) and He II photoemission measurements were set at 300 meV and 4 meV, respectively. High quality samples of $SrRu_{1-x}Ti_xO_3$ with large grain size were prepared following solid state reaction route using high purity ingredients[8] followed by a long sintering (for about 72 hours) at the final preparation temperature. Sharp x-ray diffraction patterns reveal single phase in each composition with no signature of impurity feature. Magnetic measurements using a high sensitivity vibrating sample magnetometer exhibit distinct ferromagnetic transition at each x up to $x = 0.6$ studied, as also evidenced by the Curie-Weiss fits in the paramagnetic region. The fits provide an estimation of effective magnetic moment (μ = 2.8 μ_B, 2.54 μ_B, 2.45 μ_B, 2.18 μ_B, 2.19 μ_B, 1.95 μ_B and 1.93 μ_B) and Curie temperature (θ_P = 164 K, 156.6 K, 150.6 K, 145.3 K, 139 K, 138.6 K and 100 K) for x = 0.0, 0.15, 0.2, 0.3, 0.4, 0.5 and 0.6, respectively. The values of μ and θ_P for $SrRuO_3$ are observed to be the largest among those available in the literature and corresponds to well characterized single crystalline materials[9].

In Fig. 1(a), we show the XP valence band spectra exhibiting 4 distinct features marked by A, B, C and D. The features C and D appear beyond 2.5 eV and have large O $2p$ character as confirmed experimentally

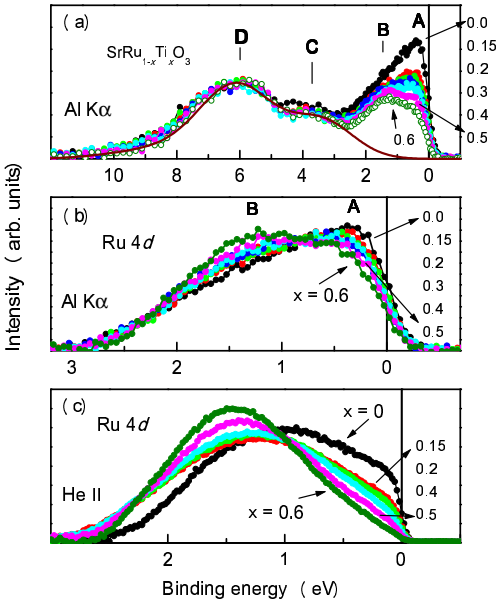

FIG. 1: (color online) (a) XP valence band spectra of $SrRu_{1-x}Ti_xO_3$ for various values of x. Solid line represents the O $2p$ part for $x = 0.6$. (b) Ru $4d$ spectra after the subtraction of the O $2p$ contributions as shown in (a). (c) Ru $4d$ band obtained from He II spectra.

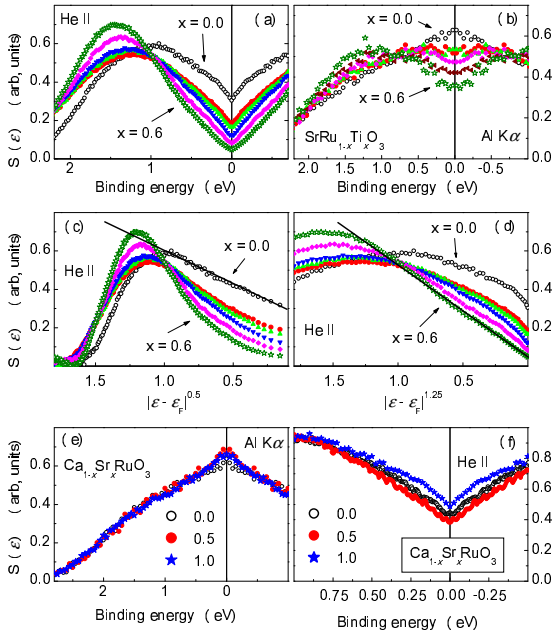

FIG. 2: (color online) $S(\epsilon)$ obtained from (a) He II and (b) XP spectra of $SrRu_{1-x}Ti_xO_3$. (b) $S(\epsilon)$ in (a) are plotted as a function of (c) $|\epsilon - \epsilon_F|^{0.5}$ (d) and $|\epsilon - \epsilon_F|^{1.25}$. $S(\epsilon)$ obtained from (e) XP and (f) He II spectra of $Ca_{1-x}Sr_xRuO_3$.

by changing photoemission cross-sections [10] and theoretically by band structure calculations [11]. The peaks A and B appear primarily due to the photoemission from electronic states having Ru $4d$ character. The O $2p$ part remains almost the same in the whole composition range as expected. While Ru $4d$ intensity gradually diminishes with the decrease in Ru-concentrations, the lineshape of Ru $4d$ band exhibits significant redistribution in intensity. In order to bring out the clarity, we delineate the Ru $4d$ band by subtracting O $2p$ contributions. The subtracted spectra, normalized by integrated intensity under the curve, exhibit two distinct features as evident in Fig. 1(b). The feature A corresponds to the delocalized electronic density of states (DOS) observed in *ab initio* results and is termed as *coherent feature*. The feature B, absent in the *ab initio* results[11], is often attributed to the signature of correlation induced localized electronic states forming the lower Hubbard band and is known as *incoherent feature*. The increase in x leads to a decrease in intensity of A and subsequently, the intensity of B grows gradually. Since the bulk sensitivity of valence electrons at 1486.6 eV photon energy is high ($\sim 60\%$), the spectral evolution in Fig. 1(b) manifests primarily the changes in the bulk electronic structure.

In order to discuss the effect due to the surface electronic structure, we show the Ru $4d$ contributions extracted from the He II spectra in Fig. 1(c), where the surface sensitivity is about 80%. Interestingly, all the spectra are dominated by the peak at higher binding energies (> 1 eV) corresponding to the surface electronic structure as reported in the case of $SrRuO_3$ and the coherent feature intensity corresponds essentially to the bulk electronic structure[10, 12]. The coherent feature intensity reduces drastically with the increase in x and becomes almost negligible at $x = 0.6$. This can be visualized clearly in the spectral density of states (SDOS) obtained by symmetrizing ($S(\epsilon) = I(\epsilon) + I(-\epsilon)$; $I(\epsilon) =$ photoemission spectra, $\epsilon =$ binding energy) the He II and XP spectra. The SDOS corresponding to He II spectrum of $SrRuO_3$ shown in Fig. 2(a) exhibits a sharp dip at ϵ_F, which increases gradually with the increase in x. The SDOS corresponding to XP spectra in Fig. 2(b), however, exhibits a peak in $SrRuO_3$ presumably due to large resolution broadening and intense coherent feature. This peak loses its intensity and becomes almost flat for $x = 0.15$ and 0.2. Further increase in x leads to a *pseudogap* at ϵ_F, which gradually increases with the increase in x. Both these results clearly indicate gradual depletion of SDOS at ϵ_F with the increase in Ti-substitution.

The effect of resolution broadening of 4 meV in the He II spectra is not significant in the energy scale shown in the figure. The electron and hole lifetime broadening is also negligible in the vicinity of ϵ_F. Thus, $S(\epsilon)$ in Fig. 2(a) provide a good testing ground to investigate evolution of the spectral lineshape at ϵ_F. The lineshape of $S(\epsilon)$ in Fig. 2(a) exhibits significant modification with the increase in x. We, thus, replot $S(\epsilon)$ as a function of $|\epsilon - \epsilon_F|^\alpha$ for various values of α. Two extremal cases representing $\alpha = 0.5$ and 1.25 are shown in Fig. 2(c) and 2(d), respectively. It is evident that $S(\epsilon)$ of $SrRuO_3$ ex-

hibit a straight line behavior in Fig. 2(c) suggesting significant role of disorder in the electronic structure. The influence of disorder can also be verified by substitutions at the A-sites in the ABO_3 structure. This has been verified by plotting SDOS obtained from the XP and He II spectra of $Ca_{1-x}Sr_xRuO_3$ in Fig. 2(e) and 2(f), respectively. Here, the electronic properties of the end members, $SrRuO_3$ and $CaRuO_3$ are known to be strongly influenced by the disorder[13]. Substitution of Sr at the Ca-sites is expected to enhance the disorder effect. The lineshape of $S(\epsilon)$ in both Fig. 2(e) and 2(f) remains almost the same across the whole composition range. Such disorder induced spectral dependence is consistent with the observations in other systems[14, 15] as well.

Interestingly, the lineshape modifies significantly with the increase in x and becomes 1.25 in the 60% Ti substituted sample. Ti substitution introduces defects in the Ru-O network, where Ti^{4+} having no d-electron, does not contribute in the valence band. Thus, in addition to the disorder effects, the reduced degree of Ru-O-Ru connectivity leads to a decrease in bandwidth, W, which in turn enhances U/W. In systems consisting of localized electronic states in the vicinity of ϵ_F, a soft Coulomb gap opens up due to electron-electron Coulomb repulsion; in such a situation, the ground state is stable with respect to single-particle excitations, when SDOS is characterized by $(\epsilon - \epsilon_F)^2$-dependence [16, 17]. Here, gradual increase in α with the increase in x in the intermediate compositions is curious and indicates strong interplay between correlation effect and disorder in this system.

The extraction of surface and bulk spectra requires both the XP and He II spectra collected at significantly different surface sensitivities. Thus, we broaden the He II spectra upto 300 meV and extract the surface and bulk spectra analytically using the same parameters as used before for $CaSrRuO_3$ system[10]. The surface spectra shown in Fig. 3(b) exhibit a gradual decrease in coherent feature intensity with the increase in x and subsequently, the feature around 1.5 eV becomes intense, narrower and slightly shifted towards higher binding energies. The decrease in intensity at ϵ_F is clearly visible in the symmetrized spectra, $S(\epsilon)$ shown in Fig. 3(d). Interestingly, $S(\epsilon)$ of $x = 0.5$ sample exhibits a soft gap at ϵ_F and a hard gap appears in $S(\epsilon)$ corresponding to higher x. This spectral evolution is remarkably consistent with the transport properties[7]. These results corresponding to 2-dimensional surface states presumably have strong implication in realizing recent theoretical predictions[1, 2, 3, 4] and the bulk properties of this system.

The picture is strikingly different in the bulk spectra where the electronic structure is 3-dimensional. The bulk spectrum of $SrRuO_3$ exhibits an intense and sharp coherent feature in the vicinity of ϵ_F and the incoherent feature appears around 2 eV. The enhancement of U/W due to Ti substitution is expected to increase the incoherent feature intensity. In sharp contrast, the intensity of the

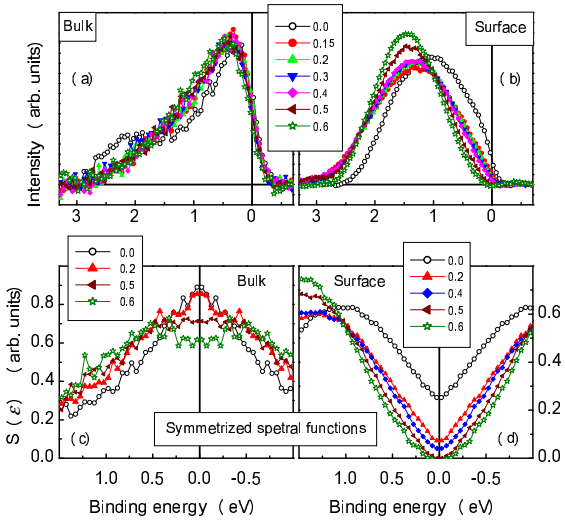

FIG. 3: (color online) Extracted (a) bulk and (b) surface spectra of $SrRu_{1-x}Ti_xO_3$ for various values of x. The SDOS obtained from bulk and surface spectra are shown in (c) and (d), respectively.

2 eV feature reduces significantly and the coherent feature becomes broad. In addition, the bulk spectra of all the intermediate compositions appear very similar. The symmetrized bulk spectra shown in Fig. 3(c) exhibit a small lowering of intensity at ϵ_F with the increase in x.

Since, U is weak in these highly extended $4d$ systems[10, 12], a perturbative approach may be useful to understand the role of electron correlation in the spectral lineshape. We have calculated the bare density of states (DOS) for $SrRuO_3$ and $SrRu_{0.5}Ti_{0.5}O_3$ using state-of-the-art full potential linearized augmented plane wave method[11, 18]. The self energy and spectral functions were calculated using this t_{2g} partial DOS as done before[19]. The real and imaginary parts of the self energy are shown in Fig. 4(a) and 4(b), and the spectral functions for different U values are shown in Fig. 4(c) and 4(d) for $SrRuO_3$ and $SrRu_{0.5}Ti_{0.5}O_3$, respectively. The increase in U leads to a spectral weight transfer outside the LDA DOS width creating the lower and upper Hubbard bands. Subsequently, the total width of the LDA DOS diminishes gradually. While these results exhibit similar scenario as that observed in the most sophisticated calculations using dynamical mean field theory, the separation between the lower and upper Hubbard bands is significantly larger than the corresponding values of U. It is important to note here that the band structure calculations include the electron-electron interaction term within the local density approximations. The perturbation calculations in the present case essentially provide an estimation of the correction in U already included in the effective single particle Hamiltonian.

In order to compare with the experimental spectra, the

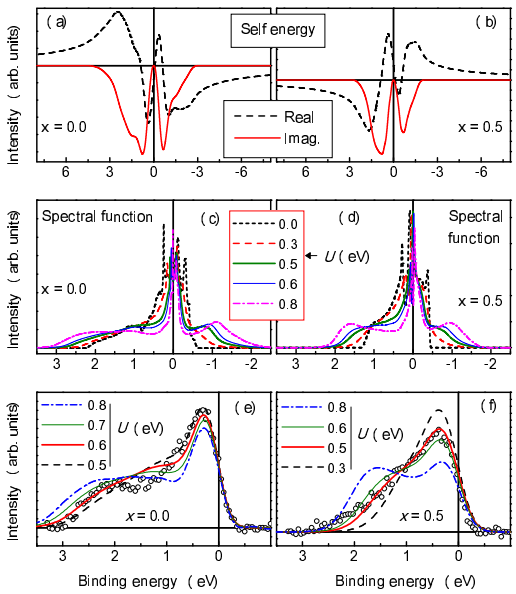

FIG. 4: (color online) Real and imaginary parts of the self energy of (a) $SrRuO_3$ and (b) $SrRu_{0.5}Ti_{0.5}O_3$ obtained by second order perturbation method following the method of Treglia *et al.*[19]. Spectral functions for various values of U of (c) $SrRuO_3$ and (d) $SrRu_{0.5}Ti_{0.5}O_3$. Calculated experimental spectra for different values of U of (e) $SrRuO_3$ and (f) $SrRu_{0.5}Ti_{0.5}O_3$.

calculated spectral functions are convoluted by Fermi-Dirac distribution function and the gaussian representing the resolution broadening of 300 meV. The comparison is shown in Figs. 4(e) and 4(f). Interestingly, the spectral shape corresponding to $U = 0.6 \pm 0.1$ exhibits remarkable representation of the experimental bulk spectra in both the cases. These results clearly establish that perturbative approaches and local description of the correlation effects are sufficient to capture electronic structure of these weakly correlated systems. The overall narrowing of the valence band observed in the substituted compounds are essentially a single particle effect and can be attributed to the reduced degree of Ru-O-Ru connectivity in these systems. While the high energy scale features are reproduced remarkably well within this picture, the occurrence of a *pseudogap* at ϵ_F with increasing x (not visible in Fig.4 due to large energy scale) suggests increasing role of disorder.

In summary, the high resolution spectra of $SrRuO_3$ exhibit signature of disorder in the vicinity of the Fermi level. Introduction of the Ti^{4+} sublattice within the Ru^{4+} sublattice provides a paradigmatic example, where the charge density near Ti^{4+} sites is close to zero and each Ru^{4+} site contributes 4 electrons in the valence band. Such large charge fluctuation leads to a significant change in spectral lineshape and a dip appears at ϵ_F (*pseudogap*). Interestingly, the effects are much stronger in the two dimensional (surface) electronic structure leading to a soft gap at 50% substitution and eventually a hard gap appears. Bulk electronic structure (3-dimensional), however, remains less influenced. A theoretical understanding of these effects needs consideration of strong disorder in addition to the electron correlation effects.

* Corresponding author: kbmaiti@tifr.res.in

[1] A. Fuhrmann, D. Heilmann, and H. Monien, Phys. Rev. B **73**, 245118 (2006).

[2] S.S. Kancharla and E. Dagotto, Phys. Rev. Lett. **98**, 016402 (2007).

[3] Arti Garg, H.R. Krishnamurthy, and Mohit Randeria, Phys. Rev. Lett. **97**, 046403 (2006).

[4] N. Paris, K. Bouadim, F. Hebert, G.G. Batrouni, and R.T. Scalettar, Phys. Rev. Lett. **98**, 046403 (2007).

[5] J. Kim, J.-Y. Kim, B.-G. Park, and S.-J. Oh, Phys. Rev. B **73**, 235109 (2006), M. Abbate, J.A. Guevara, S.L. Cuffini, Y.P. Mascarenhas, and E. Morikawa, Eur. Phys. J. B **25**, 203 (2002).

[6] S. Ray, D.D. Sarma, and R. Vijayaraghavan, Phys. Rev. B **73**, 165105 (2006).

[7] K.W. Kim, J.S. Lee, T.W. Noh, S.R. Lee, and K. Char, Phys. Rev. B **71**, 125104 (2005).

[8] R.S. Singh and K. Maiti, Solid State Commun, **140**, 188 (2006).

[9] G. Cao, S. McCall, M. Shepard, J.E. Crow, and R.P. Guertin, Phys. Rev. B **56**, 321 (1997).

[10] K. Maiti and R.S. Singh, Phys. Rev. B **71**, 161102(R) (2005).

[11] K. Maiti, Phys. Rev. B **73**, 235110 (2006).

[12] M. Takizawa, D. Toyota, H. Wadati, A. Chikamatsu, H. Kumigashira, A. Fujimori, M. Oshima, Z. Fang, M. Lippmaa, M. Kawasaki, and H. Koinuma, Phys. Rev. B **72**, 060404(R) (2005).

[13] K. Maiti, R.S. Singh, and V.R.R. Medicherla, Europhys. Lett. (in print); Condmat/0604648.

[14] B.L. Altshuler and A.G. Aronov, Solid State Commun. **30**, 115 (1979).

[15] D.D. Sarma *et al.*, Phys. Rev. Lett. **80**, 4004 (1998).

[16] A.L. Efros and B.I. Shklovskii, J. Phys. C: Solid State Phys. **8**, L49 (1975).

[17] J.G. Massey and M. Lee, Phys. Rev. Lett. **75**, 4266 (1995).

[18] P. Blaha, K. Schwarz, G.K.H. Madsen, D. Kvasnicka, and J. Luitz, WIEN2k, An Augmented Plane Wave + Local Orbitals Program for Calculating Crystal Properties (Karlheinz Schwarz, Techn. Universität Wien, Austria), 2001. ISBN 3-9501031-1-2.

[19] G. Treglia *et. al.*, J. Physique **41**, 281 (1980); *ibid*, Phys. Rev. B **21**, 3729 (1980); D.D. Sarma *et al.*, Phys. Rev. Lett. **57**, 2215 (1986).